

This article appeared in a journal published by Elsevier. The attached copy is furnished to the author for internal non-commercial research and education use, including for instruction at the authors institution and sharing with colleagues.

Other uses, including reproduction and distribution, or selling or licensing copies, or posting to personal, institutional or third party websites are prohibited.

In most cases authors are permitted to post their version of the article (e.g. in Word or Tex form) to their personal website or institutional repository. Authors requiring further information regarding Elsevier's archiving and manuscript policies are encouraged to visit:

<http://www.elsevier.com/copyright>



Contents lists available at ScienceDirect

Optics & Laser Technology

journal homepage: [www.elsevier.com/locate/optlastec](http://www.elsevier.com/locate/optlastec)



# Effective removal of adhering cells via ultrashort laser pulses

Xiaoliang Wang, Zhixiong Guo<sup>\*</sup>

Department of Mechanical and Aerospace Engineering, Rutgers, the State University of New Jersey, 98 Brett Road, Piscataway, NJ 08854, United States

## ARTICLE INFO

### Article history:

Received 20 January 2009

Received in revised form

19 August 2009

Accepted 20 August 2009

Available online 6 September 2009

### Keywords:

Plasma-mediated laser ablation

Cell removal

Surface decontamination

## ABSTRACT

A technique for accurately and effectively removing adhering red blood cells in a blood plasma thin film via a picosecond pulsed laser was developed. The laser beam was focused to the surface of the film to generate plasma-mediated ablation and an automated stage was employed for raster scan. The SEM images showed that the red blood cells distributed in the ablation scanned area were removed neatly, leaving the surroundings and the film base intact. For cells across the boundary between the ablated and untreated areas, a trim cutting interface was observed. Complete ablation of red blood cells in the target area is achieved without visible thermal and collateral damage in the remaining structure. The removal method is very effective because it is not necessary to selectively focus a laser beam on individual target cells and remove cells one by one. The ablation is scanned over a certain size of area, enabling practical cell killing or microbial decontamination in clinical/industrial scale.

© 2009 Elsevier Ltd. All rights reserved.

## 1. Introduction

Ultrashort pulsed (USP) laser technology has emerged as a promising method for material machining and surface processing since its advent in the middle 80's of last century, owing to its unique interaction mechanism with material that is different from conventional continuous-wave (CW) and nanosecond-pulsed lasers. When the extremely short pulse of laser is converged to a small focal volume, the energy flux is so high that it induces optical breakdown, taking material away within the focal volume via plasma-mediated ablation. The substantial plasma absorption enables the ablation of materials that are normally difficult to ablate by conventional lasers, such as transparent or low absorption materials [1,2]; and the ablation does not depend on the laser wavelength and material absorption property. Extensive studies utilizing USP laser ablation in basic science and industrial applications have been carried out [3,4]. In recent years, USP lasers have attracted increasing attention in biomedicine, including imaging of early cancers [5,6], human chromosomes dissection [7], and ablation of soft and hard tissues [8–10].

Nowadays a great number and diverse types of expensive, intricate instruments and implants are used in the hospital and clinical environment. Historically, sterilization was done mainly through physical methods, especially using moist heat in the form of steam autoclaves as well as dry heat. Alternative technologies are needed while high heat wet or dry is not an option for all instruments.

Removal of unwanted materials, especially contaminants, from the surface of allograft, xenograft, and autograft tissues is important for preparing the tissue for implantation. However, there are few methods that can effectively remove unwanted material without harming or damaging the tissue [11]. Common methods like applying solutions comprising peracetic acid, povidone-iodine, or mixtures of antibiotics produce large quantity of liquid which are polluting or environmentally unfriendly. Gamma irradiation can alter the structural and biomechanical properties of the tissue. Therefore, it would be useful to develop an effective method of removing unwanted materials and contaminants from the surface of graft tissues without damaging or altering the properties of the tissue.

Microorganisms present upon the surfaces of apparatus and tissues easily form a thin biofilm. Adhesion forces make biofilms difficult to eliminate by detergents and mechanical action [12]. Bacteria in biofilms are more resistant to treatment with disinfectants than bacteria suspended in liquid media. Recently, Sadoudi et al. [13] assessed the efficacy of nanosecond-pulsed laser beams (1064, 532 and 355 nm, and 20 ns pulses) for removal and killing of adherent bacteria from stainless steel surfaces. Non-intrusive and precise processing makes lasers superior in surface decontamination.

Cell ablation is usually employed to study cell lineage or function by selectively destroying a small number of cells. It can also be considered as a tumor therapy. For example, Clark et al. [14] used nitroreductase-mediated inducible cell ablation for the selective killing of cells *in vivo*. It is known that radiofrequency ablation, in which a probe releases a high-frequency current that heats the tumor and destroys the cancer cells, has become a promising treatment method for small tumors [15]. Certainly a laser beam can also be utilized to focus on and kill target cells.

<sup>\*</sup> Corresponding author. Tel.: +1732 445 2024.

E-mail address: [guo@jove.rutgers.edu](mailto:guo@jove.rutgers.edu) (Z. Guo).

Recently, the inactivation of viruses such as M13 bacteriophages subject to excitations of a visible femtosecond laser has been studied by Tsen et al. [16]. In the cell ablation methods mentioned above, ablation only referred to local killing or inactivation of cells.

In this article, we demonstrate a new technique for the removal of unwanted adhering cells via USP laser pulses using red cells in a plasma film as an example. A survey of literature reveals that no similar work has been done before. The distinct features of this methodology include: (1) the ablation of the cells in the ablated area is complete and accurate, leaving the surroundings and substrate beneath the cells intact although these regions are also laser ablation scanned; (2) there is no visible thermal and collateral damage in the remaining structure; (3) the laser beam scans over a target surface and it is not necessary to selectively focus on the target cells only, enabling practical cell killing and microbial decontamination in clinical/industrial scale.

## 2. Material and methods

Fig. 1 shows the schematic sketch of the experimental setup and a photo of the laser beam focus lens and lab-fabricated sample fixture. An erbium-doped fiber laser (Raydiance, Inc.) was used in the experiment. The laser outputs pulses at wavelength 1552 nm with pulse duration of 1.2 ps. Its repetition rate is tunable between 1 Hz and 500 kHz. The pulse energy is also adjustable between 1 and 5  $\mu$ J. A computer was used to control and monitor

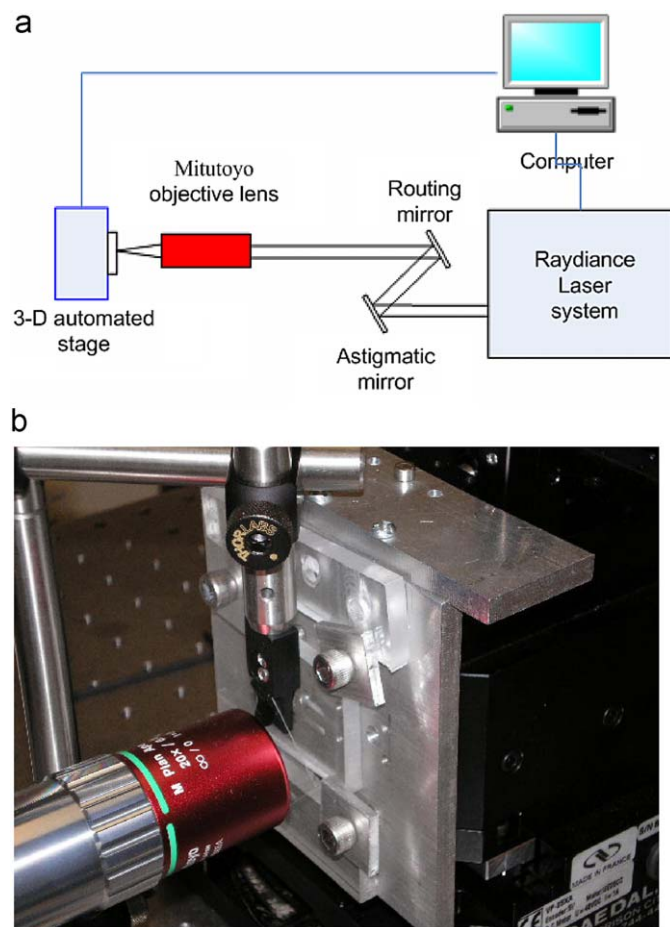


Fig. 1. (a) Sketch of the experimental setup and (b) photo of the focus lens and sample fixture.

the pulse repetition rate and output energy. The laser beam was modified by an astigmatism correction mirror before it was launched into a long working distance objective lens (M Plan Apo NIR 20  $\times$  /0.4 N.A., Mitutoyo). For a beam of Gaussian spatial distribution, its focal spot diameter ( $1/e^2$ ) can be calculated by  $d = 2.44\lambda f/\phi$ . For the current laser and beam delivery system, the wavelength  $\lambda$  is 1552 nm; the focal length  $f$  is 20 mm; and the beam diameter before the lens  $\phi$  is approximately 10 mm. Therefore, the calculated focal spot size is 7.6  $\mu$ m in diameter. The actually measured spot size is about 8.0  $\mu$ m in free space. A digital power meter was used to measure the laser power transmission loss in the objective lens and the loss was 49%. Such a transmission loss in the lens has been accounted for in the fluence values stated hereafter.

Blood is a very common type of contamination present to the surface of surgical devices and allograft, xenograft, and autograft tissues. In the current study, sheep whole blood with anticoagulant citrate (Hemostat Laboratories) was adopted. The sheep whole blood was preserved in a refrigerator at 4  $^{\circ}$ C. To prepare for experimental samples, the blood was smeared onto the surface of microscopic slide and exposed in air at room temperature for several hours. After the blood became dry, a film of blood stain would be formed on the slide surface. Two types of samples were considered, depending on the thickness of the blood film. When the blood plasma film thickness was well controlled under 1  $\mu$ m, one could obviously observe that many individual red blood cells adhere in and top the plasma film (see the cylindrical plates in Fig. 3). This is because the whole blood contains a high volume percentage (up to 45%) of blood cells, mainly red blood cells (erythrocytes). The plasma base film is composed of plasma proteins and chemicals. We used this type of thin film samples to demonstrate the removal of adhering cells in biofilms in this study. When the thickness of the blood film was over 3–4  $\mu$ m, individual blood cells topping the film were hardly distinguishable and the blood was formed into clots (see Fig. 2). We used this type of thick film samples in the demonstration of removal of a layer or multiple layers of contaminations.

Before experiment the sample was placed to a custom-made altitude-adjustable sample fixture which was hold to a programmable 3-D automated precision compact linear stage (VP-25XA, Newport) controlled by the computer. We kept the sample slide flat on the fixture and aligned it with the focused beam through moving the stage along the optical axis (z-direction). When a brilliant green spark (third harmonic of the 1552 nm laser) is observed at the sample surface, plasma-mediated ablation occurs and the working distance is fixed. After that, the automated stage was moved in the x-y plane to let the focal spot impinge on the film surface. The stage can also be moved in a pre-programmed pattern to have a raster scan of the focused beam on a selective area of the sample surface. To collect the aerosols formed from the ablated material, an extraction vacuum (FX225, EDSYN) was used and the extraction nozzle was pointed at the sample surface with about 3 cm clearance.

The micro topography of the ablated surfaces were observed and characterized with an upright digital microscope (National Optical DC3-156-S) and a scanning electron microscopy (SEM, AMRAY 1830I).

## 3. Results and discussion

Fig. 2 shows microscopic view of the decontamination results on a blood film sample about 3.5  $\mu$ m thick (measured by a stylus profiler, Dektak 3030). Three ablation stripes of dimension 1 by 20 mm were scanned with different laser pulse energies. During the scanning, continuous green sparks at the film surface were



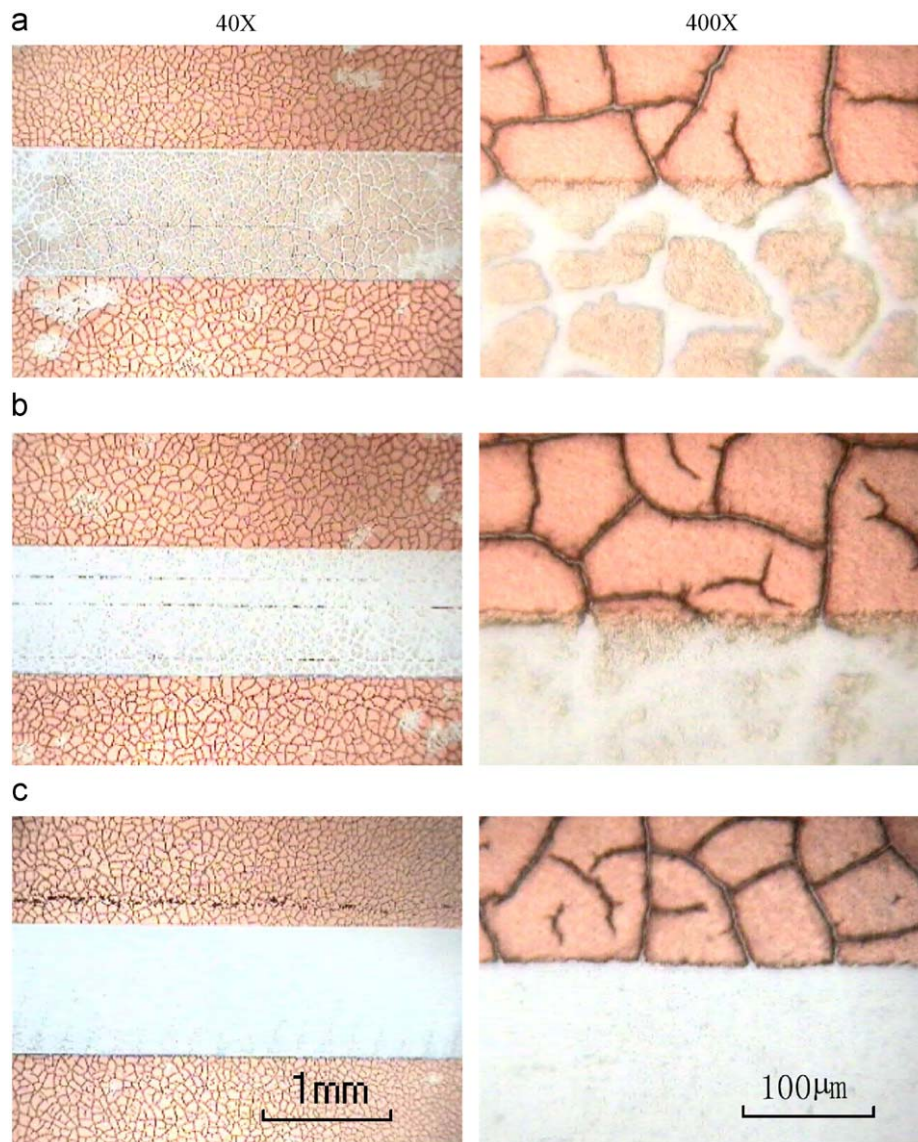


Fig. 2. Microscopic views of ablation stripes with different pulse fluence values: (a) 2.07 J/cm<sup>2</sup>; (b) 3.07 J/cm<sup>2</sup>; and (c) 4.54 J/cm<sup>2</sup>.

observed. When the computer reading for the laser output was set at 2.0 µJ per pulse, the actual incident pulse energy on the sample was 1.04 µJ due to the 49% transmission loss in the focus lens. It corresponds to an averaged fluence of 2.07 J/cm<sup>2</sup> in the Gaussian beam focal spot (8 µm in diameter). It should be noticed that the fluence values used thereafter are the averaged pulse fluence in the beam focal spot, if not otherwise specified. Before the raster area scan, we characterized the ablation line width which is generally 6–10 µm wide. However, the strips were scanned with ablation lines 2 µm apart to ensure better area ablation effect by eliminating ablation inconsistency caused by factors such as vibration and wavy motion of the work stage, surface morphology variation, etc. The automated stage moved in the x–y plane with a velocity of 20 mm/s and the pulse repetition rate is 20 kHz. Thus, the pulse overlap rate is 1 pulse/µm along the ablation advancing line.

When the pulse fluence is low (e.g., 2.07 J/cm<sup>2</sup>), it is found from Fig. 2(a) that the ablation depth is shallow. Only a top layer of the blood contamination film is removed and the clots in the contamination film are clearly observable in both the 40× and 400× magnification images. When the pulse fluence is increased to 3.07 J/cm<sup>2</sup>, the 40× magnification image in Fig. 2(b) shows that the decontamination in the scanned strip is almost gone.

However, clots yet exist in the enlarged 400× view in Fig. 2(b). The optimal removal result is obtained with the pulse fluence 4.54 J/cm<sup>2</sup> in Fig. 2(c), where both the 40× and 400× magnification images display complete removal of the whole blood film from the slide surface. There are no melting/solidification and charring marks in the images in Fig. 2. It proves that the ablation is plasma-mediated, not based on the conventional thermal ablation mechanism. Thus, thermal damage is eliminated or minimized. Further, no crack is observed in the surrounding blood stain and in the slide substrate. Hence, there is no collateral mechanical damage.

The objective of this study is to demonstrate a technique for removing unwanted cells or other tiny contaminant like bacteria, yeasts, and fungi from the surface of allograft, xenograft, and autograft tissues. We use the thin blood film as an example, in which the adhering red blood cells represent the unwanted cells or contaminant and the plasma film base stands for the tissue. The results in Fig. 2 have revealed that a low pulse fluence of 2.07 J/cm<sup>2</sup> is preferred for removing unwanted adhering cells in a blood plasma film without damaging the film substrate.

Fig. 3 shows some cell removal pictures taken by the SEM. In Fig. 3(a), untreated red blood cells (the cylindrical plates)

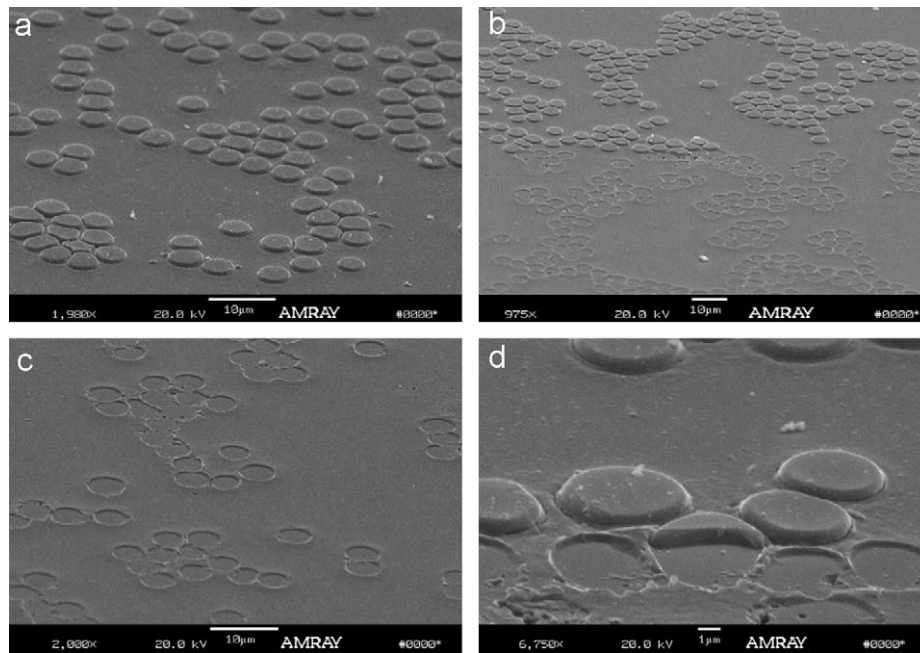


**Fig. 3.** SEM pictures showing removal of red blood cells: (a) view of part of the untreated area; (b) view of both the ablated and untreated areas at  $975\times$  magnification; (c) view of part of the ablated area at  $2000\times$  magnification; and (d) view of the boundary across the ablated and untreated areas at  $6750\times$  magnification.

adhering in and topping on a thin plasma film are illuminated at  $1980\times$  magnification. It is estimated from the SEM image that the diameter of the red blood cells is around  $7\mu\text{m}$  and the thickness of the dry cell plates in the film is about  $0.5\mu\text{m}$  (estimated from the enlarged view in Fig. 3(d)). The incident pulse fluence was  $2.07\text{J}/\text{cm}^2$ ; and thus, had a peak value of  $4.14\text{J}/\text{cm}^2$  in the spot center. This peak value is lower than the ablation threshold,  $9.65\pm 1.21\text{J}/\text{cm}^2$ , for human dermal tissue that is very commonly used in tissue transplantation [9]. Therefore, it will not cause plasma-mediated ablation in the substrate tissue. To generate a complete cell removal pattern in the strip, the automated work stage was moved at  $20\text{mm/s}$  in the  $y$ -direction and the pulse repetition rate was set at  $20\text{kHz}$ . Successive ablation lines  $2\mu\text{m}$  apart in the  $x$ -direction were performed so that the overlap of the lines can achieve good area ablation effect. Green ablation sparks were observed above the film surface during the scanning. The brightness of the sparks is relatively weak as compared to the case for Fig. 2(a).

Fig. 3(b) is a view at  $975\times$  magnification of both the ablated and untreated cell regions in a boundary of the scanning strip. It is seen that all the cells within the ablated area (the bottom half in the picture) are removed very neatly, while all the cells in the untreated area are intact. Fig. 3(c) is an amplified view of part of the ablated area at  $2000\times$  magnification. The round craters in the picture are the foot prints left by the ablated cells in the blood thin film. The cells were very neatly removed from the biofilm, as if someone removed them one by one using a precise tool. Surprisingly both the blood plasma films beneath and surrounding the cells were not ruined; neither was mechanical and thermal damage observed.

Fig. 3(d) displays an interface between the ablated strip and the untreated area at  $6750\times$  magnification. From this photo it is observed that for the cell across the interface, a very clear and sharp cut separated the cell into two parts. The part of the cell within the ablation regime is completely gone. However, the remaining part still retains its own structure. There is no any visible crack or collateral damage in the remaining half cell. Further inspection of several other cells across such an interface substantiated this finding.

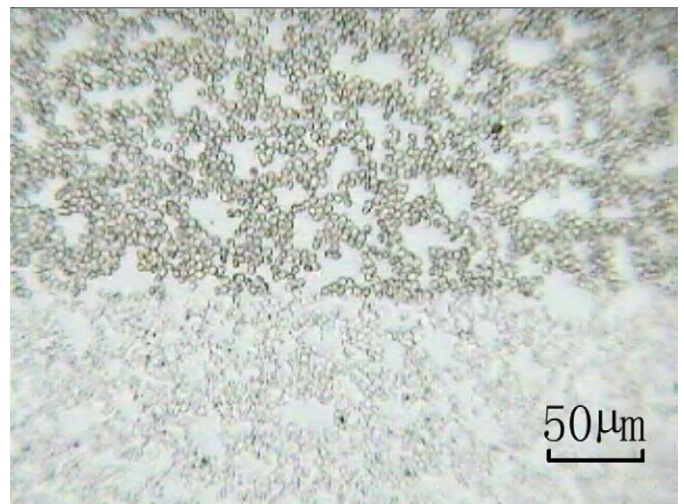


**Fig. 4.** Digital microscopic image showing part of the ablated area (bottom half) and part of the untreated area (top half) at  $400\times$  magnification.

Fig. 4 is a view of relatively large area under a general-purpose digital microscopy at  $400\times$  magnification. A clear interface separates the ablated and untreated regions. The result in the ablated area further confirms that all the cells in the treated strip are neatly removed.

It is worth mentioning an interesting phenomenon observed. That is the cell including its “root” embedded in the base film was gone as a whole, while the surrounding film that has a higher altitude than the ablated cell “root” remained untouched even though the surroundings were also laser-scanned. The laser beam was well controlled such that there was no ablation to the level at the plasma base film. Thus, it is clear that the removal of the cell “root” was not due to direct laser irradiation. There are probably two causes: (1) the generated plasma during the ablation of the top part of the cell penetrated into the “root”; and (2) the mechanical force associated with the ablation was efficient to overcome the adhesion, but not sufficient to cause structural



damage. It is evident that collateral damage is invisible because the remaining half cell as shown in Fig. 3(d) is solid in the film. Although mechanical damage is not found in the current study, it is worth mentioning that previous studies in plasma-mediated ablation have demonstrated that, when the incident pulse flux is over another threshold in optical breakdown, mechanical damage because of shock wave generation and plasma cavitations should be concerned.

The present research is of significance in a broad field requiring removal of unwanted cells or contaminants from a surface without collateral and thermal damage. For example, allograft tissues and matrices often have to be modified before implantation. This includes removing unwanted cells such as the viable cells in skin grafts. Techniques using a mechanical cutter or surgical knife are often imprecise and can result in damage to the underlying layers or surrounding tissue. Ablation techniques based on radiofrequency or traditional pulsed lasers can generate substantial heat during application, which can be transferred to the surrounding tissue and may result in coagulation or charring of the tissue.

Another potential application is the removal of unwanted stem cells, such as the elimination of undifferentiated human embryonic stem (hES) cells [17]. There is a risk associated with the transplantation of differentiated hES cells to patients as undifferentiated hES cells are potentially tumorigenic and may be within heterogeneous populations of differentiated cells. Current strategies to eliminate specific cell types such as the use of the thymidine kinase gene to confer sensitivity to Gancyclovir could result in death of wild-type cells by means of the “bystander effect” [18]. Because only individual cells within the local volume would be ablated as demonstrated in the present study, undifferentiated hES cells might be removed without causing death of wild-type cells via the USP laser plasma-mediated ablation technique.

#### 4. Conclusion

Complete and effective removal of only cells adhered in the target area is realized via the plasma-mediated ablation scan using a picosecond laser. No thermal and collateral damage is observed to the surroundings and the underlying base film. For cells across the boundary between the ablated and untreated areas, the part in the scanned area is trimmed while the part in the untreated area retains its structure, resulting in a neat cutting interface. This laser removal method is very effective because it is not necessary to selectively focus a laser beam on individual target cells. The ablation is scanned over a certain size of area,

enabling practical cell killing or microbial decontamination in clinical/industrial scale. Removal of a thick layer of blood stain is also demonstrated.

#### Acknowledgements

Support of this work by the Musculoskeletal Transplant Foundation and Raydiance, Inc., is gratefully acknowledged. The SEM measurement was conducted by lab member Huan Huang.

#### References

- [1] Hwang D, Choi T, Grigoropoulos CP. Liquid-assisted femtosecond laser drilling of straight and three-dimensional microchannels in glass. *Appl Phys A* 2004;79:605–12.
- [2] Huang H, Guo Z. Ultra-short pulsed laser PDMS thin-layer separation and micro-fabrication. *J Micromech Microeng* 2009;19:055007.
- [3] Aguilar CA, Lu Y, Chen SC. Micro-patterning of biodegradable polymers using UV and femtosecond lasers. *Biomaterials* 2005;26:7642–9.
- [4] Srisungsithisunti P, Ersoy OK, Xu X. Volume Fresnel zone plates fabricated by femtosecond laser direct writing. *Appl Phys Lett* 2007;90:011104.
- [5] Quan H, Guo Z. Fast 3-D optical imaging with transient fluorescence signals. *Opt Express* 2004;12:449–57.
- [6] Guo Z, Wan SK, August DA, Ying J, Dunn SM, Semmlow JL. Optical imaging of breast tumor through temporal log-slope difference mappings. *Comput Biol Med* 2006;36:209–23.
- [7] König K, Riemann I, Fritzsche W. Nanodissection of human chromosomes with near-infrared femtosecond laser pulses. *Opt Lett* 2001;26:819–21.
- [8] Niemz MH, Klancnik EG, Bille JF. Plasma-mediated ablation of corneal tissue at 1053 nm using a Nd:YLF oscillator/regenerative amplifier laser. *Lasers Surg Med* 1991;11:426–31.
- [9] Huang H, Guo Z. Human dermis separation via ultra-short pulsed laser plasma-mediated ablation. *J Phys D: Appl Phys* 2009;42:165204.
- [10] Liu Y, Niemz MH. Ablation of femoral bone with femtosecond laser pulses—a feasibility study. *Lasers Med Sci* 2007;22:171–4.
- [11] Gertzman AA and Schuler M. Private Communications, the Musculoskeletal Transplant Foundation 2007.
- [12] Boulange-Petermann L, Baroux B, Bellon-Fontaine MN. The influence of metallic surface wettability on bacterial adhesion. *J Adhesion Sci Technol* 1993;7:221–30.
- [13] Sadoudi AK, Harry JM, Cerf O. Elimination of adhering bacteria from surfaces by pulsed laser beams. *Lett Appl Microbiol* 1997;24:177–9.
- [14] Clark AJ, Iwobi M, Cui W, Crompton M, Harold G, Hobbs S, et al. Selective cell ablation in transgenic mice expression *E. coli* nitroreductase. *Gene Ther* 1997;4:101–10.
- [15] Paschos K, Bird N. Current diagnostic and therapeutic approaches for colorectal cancer liver metastasis. *Hippokratia* 2008;12:132–8.
- [16] Tsen KT, Tsen SW, Chang CL, Hung CF, Wu TC, Kiang JG. Inactivation of viruses by laser-driven coherent excitations via impulsive stimulated Raman scattering process. *J Biomed Opt* 2007;12:064030.
- [17] Schuldiner M, Itskovitz-Eldor J, Benvenisty N. Selective ablation of human embryonic stem cells expressing a “suicide” gene. *Stem Cells* 2003;21:257–265.
- [18] Hewitt Z, Priddle H, Thomson AJ, Wojtacha D, McWhir J. Ablation of undifferentiated human embryonic stem cells: exploiting innate immunity against the Gal {alpha}1-3Gal{beta}1-4GlcNAc-R ((alpha)-Gal) epitope. *Stem Cells* 2007;25:10–18.